AD-777 893

IDENTIFICATION OF KINETIC PERFORMANCE LOSSES OF NTO/MMH

Fred S. Andes, III

Air Force Rocket Propulsion Laboratory
Edwards Air Force Base, California

February 1974

UNCLASSIFIED
SECURITY CLASSIFICATION OF THIS PAGE (When Data Entered)

REPORT DOCUMENTATION PAGE		READ INSTRUCTIONS BEFORE COMPLETING FORM
1. REPORT NUMBER AFRPL-TR-73-102	2. GOVT ACCESSION NO.	3. RECIPIENT'S CATALOG NUMBER AD 777893
4. TITLE (and Subtitle) Identification of Kinetic Performance Losses of NTO/MMH		5. TYPE OF REPORT & PERIOD COVERED Final Jul 72 - 31 Aug 73 6. PERFORMING ORG. REPORT NUMBER AFRPL-TR-73-102
7. AUTHOR(s) Fred S. Andes III, Capt, USAF		8. CONTRACT OR GRANT NUMBER(s)
9. PERFORMING ORGANIZATION NAME AND ADDRESS Air Force Rocket Propulsion Laboratory LKCE Edwards, C[illegible] 93523		10. PROGRAM ELEMENT, PROJECT, TASK AREA & WORK UNIT NUMBERS JON 305810RL
11. CONTROLLING OFFICE NAME AND ADDRESS		12. REPORT DATE FEBRUARY 1974 13. NUMBER OF PAGES 45
14. MONITORING AGENCY NAME & ADDRESS(if different from Controlling Office) N/A		15. SECURITY CLASS. (of this report) UNCLASSIFIED 15a. DECLASSIFICATION/DOWNGRADING SCHEDULE N/A

16. DISTRIBUTION STATEMENT (of this Report)

APPROVED FOR PUBLIC RELEASE, DISTRIBUTION UNLIMITED

17. DISTRIBUTION STATEMENT (of the abstract entered in Block 20, if different from Report)

18. SUPPLEMENTARY NOTES

19. KEY WORDS (Continue on reverse side if necessary and identify by block number)
Kinetic losses, nozzle design, nozzle performance, area ratio, finite rate chemistry, nonequilibrium chemistry effects, kinetically designed nozzle analytical model.

20. ABSTRACT (Continue on reverse side if necessary and identify by block number)

The objective of the Kinetically Designed Nozzle in-house program was to determine whether an increase in performance could be obtained over present conventional isentropic nozzle design techniques by considering nonequilibrium chemistry effects in the design process. It was structured as a three phase program.

Phase I included a parametric study to analytically determine if there was a significant increase in nozzle performance to be gained using the Kinetically

DD FORM 1 JAN 73 1473 EDITION OF 1 NOV 65 IS OBSOLETE

Item 20 Continued

Designed Nozzle (KDN) analytical model for a general multi-component reacting gas. This computer program was written by Allan A. Taylor and Joe D. Hoffman as reported in AFAPL-TR-71-92 (Reference 1). The results of this study would then be used to decide whether to proceed to the next two phases that would entail the fabrication and testing of several nozzles. Unfortunately, the KDN computer program could not be made to work right with the NTO/MMH propellant combination and this entire effort had to be terminated short of its original goal.

This report summarizes the work done in Phase I using the JANNAF methodology to determine the kinetic performance of a 15^{0} conical nozzle and numerous Bell nozzles for a wide range of engine operating and geometrical conditions.

CONTENTS

FIGURES

TABLES

SECTION I

INTRODUCTION

An analysis of Soviet rocket nozzles, which was made openly available to the West during the last few years, has shown that they are consistently shorter and of a higher area ratio than similar US designs. This initiated the development of two new design approaches for increasing nozzle performance:

(1) The truncated nozzle method, which is used throughout the rocket industry.

(2) The more recent kinetically optimized nozzle technique, which is based on finite rate chemistry.

The second method potentially exhibits great promise of extending our ability to devise shorter, higher performing nozzles. Noticeable performance increases have been achieved analytically by using the actual non-equilibrium flow chemistry in the design process (References 1-5). This increased performance can primarily be attributed to specie recombination, which governs the amount of thermal energy release. To avoid "freezing" the flow, the finite-rate nozzle contours do not generally expand as rapidly as do isentropic nozzles. This permits the release of additional thermal energy that can be converted into directed kinetic energy for increased performance. Due to their complexity, these analytical models can be most effectively applied when there is sufficient knowledge of the range of operating conditions for which significant kinetic losses are incurred. Application of the models in this range thereby maximizes their usefulness and their ability to predict contours that can convert a performance loss into an overall performance gain. Based on this fact, a study was conducted to determine the kinetic performance of a 15^{o} conical nozzle and numerous Bell nozzles for a wide range of engine operating and geometrical conditions. The bipropellant chosen for the study was the high-energy storable liquid, nitrogen tetroxide and monomethylhydrazine,

NTO/MMH. This report summarizes the program's attempts to evaluate significant reaction mechanisms and provide guidelines for inputting subsequent finite-rate nozzle design models.

SECTION II

APPROACH

Computations of the kinetics losses for specific operating conditions can be made by employing the computer models and methodology suggested by the JANNAF Performance Standardization Working Group. The computer model used was the Two-Dimensional Kinetic Reference Program (TDK) (Reference 6) with the options for the One-Dimensional Kinetic (ODK) codes.

1. Method

The method employed is the one outlined in the JANNAF Simplified Procedure (Reference 7) assuming a single zone case with completely vaporized combustion gases at the throat plane. The engine kinetic efficiency can be expressed as

$$\eta_{\substack{Isp \\ EKL}} = \left[\left. \begin{matrix} Isp \\ ODK \\ (O/F)\ Avg \end{matrix} \right/ \begin{matrix} Isp \\ ODE \\ (O/F)\ Avg \end{matrix} \right]_{\varepsilon} \tag{1}$$

The corresponding engine specific impulse kinetics loss is then calculated by applying the relation

$$Isp_{\substack{EKL}} = \left(Isp_{ODE}\right)\left(\eta_{\substack{Isp \\ EKL}}\right) \tag{2}$$

The kinetic loss associated with the nozzle, or that which could be recovered in the nozzle region, is slightly different in magnitude than the engine kinetic loss calculated previously. This is due to kinetic losses which occur in the convergent transonic region upstream of the throat.

They can be eliminated by using the following relations:

$$\eta_{Isp} \left[\left(\begin{matrix} Isp \\ ODK \\ (O/F)\ Avg \end{matrix} \right)_{\varepsilon} - \left(\begin{matrix} Isp \\ ODK \\ (O/F)\ Avg \end{matrix} \right)_{TH} \Bigg/ \left(\begin{matrix} Isp \\ ODE \\ (O/F)\ Avg \end{matrix} \right)_{\varepsilon} - \left(\begin{matrix} Isp \\ ODE \\ (O/F)\ Avg \end{matrix} \right)_{TH} \right] \tag{3}$$

and

$$\begin{matrix} Isp \\ NKL \end{matrix} \left[\left(\begin{matrix} Isp \\ ODE \\ (O/F)\ Avg \end{matrix} \right)_{\varepsilon} - \left(\begin{matrix} Isp \\ ODE \\ (O/F)\ Avg \end{matrix} \right)_{TH} \right] \left(\begin{matrix} \eta_{Isp} \\ NKL \end{matrix} \right) \tag{4}$$

This slight modification of equations 1 and 2 is necessary because the nozzle design techniques mentioned in References 1-5 start their recontouring downstream of the throat region. Therefore, we need to know only the magnitude of the kinetic loss in the nozzle region, which is what equations 3 and 4 will give.

2. Test Matrix

Two basic nozzle designs, a 15° cone and various Bell shaped contours, were considered to determine the kinetic losses of NTO/MMH using a wide range of engine operating conditions. Table 1 summarizes the matrix over which they were exercised. The conical contour was the baseline configuration; the design point at each thrust level was a 2.5 mixture ratio, 100 psia chamber pressure and 25/1 area ratio. Contour throat radius specifics are given in Figure 1 and Table 2. The Bell contours were designed using an isentropic method of characteristics solution and are constrained to the same axial length as the conical nozzles. The normalized axial and radial coordinates and other pertinent data are given in Tables 3 and 4.

TABLE 1

VARIABLE MATRIX OF NOZZLE KINETICS ANALYSIS USING NTO/MMH

STUDY 1 - 15° CONE	
Variable Name	Variable Range
Area Ratio - ε	25, 50, 75, 100
Mixture Ratio (Ox/Fu) - MR	1.5, 2.0, 2.5, 3.0, 3.5
Chamber Pressure (psia) - Pc	50, 100, 300, 500
Thrust (lbf) - T	300, 3000, 18000
Normalized Downstream Radius of Curvature - Rc	0.5
STUDY 2 - 15° CONE	
Area Ratio - ε	1.0 - 100 (12 steps in between)
Mixture Ratio (Ox/Fu) - MR	2.5
Chamber Pressure (psia) - Pc	50, 100, 300, 500
Thrust (lbf) - T	300, 3000, 18000
Normalized Downstream Radius of Curvature - Rc	1.0, 2.0, 2.0, 5.0, 8.0, 10.0, 25.0
STUDY 3 - BELL	
Area Ratio - ε	36, 40, 45, 52, 74, 83, 94
Mixture Ratio (Ox/Fu) - MR	2.0, 2.5, 3.0
Chamber Pressure (psia) - Pc	50, 100, 300, 500
Thrust (lbf) - T	300, 3000
Normalized Downstream Radius of Curvature - Rc	0.5
% Bell	80, 75, 70, 65

TABLE 2

NOZZLE THROAT DETERMINATION

Pc (psia)	300# Thrust				3,000# Thrust				18,000# Thrust			
	50	100	300	500	50	100	300	500	50	100	300	500
Thrust Coefficient - C_F (ε = 25/1)	1.816	1.824	1.836	1.849	1.826	1.838	1.856	1.861	1.861	1.841	1.867	1.8711
Characteristic Velocity C* (ft/sec)	5436	5455	5543	5578	5436	5455	5443	5578	5436	5455	5543	5578
Mass Mixture Ratio - MR	2.5	2.5	2.5	2.5	2.5	2.5	2.5	2.5	2.5	2.5	2.5	2.5
Throat Area - A_t in.^{2}	4.4693	2.242	0.7482	0.4489	33.251	16.764	5.538	3.310	199.98	100.59	33.23	19.862
Throat Radius - R_t in.	1.1927	0.8452	0.488	0.378	3.2533	2.310	1.3277	1.0265	7.9785	5.6584	3.2522	2.5144
Mass Flowrate $\dot{m}$ (lbm/sec)	1.339	1.3284	1.3237	1.300	9.909	9.886	9.663	9.573	59.40	59.23	57.84	57.20

P_c = 100 psia A_t = 2.242 in^2
$\dot{w}$ = 1.328 lbm/sec R_t = 0.8452"

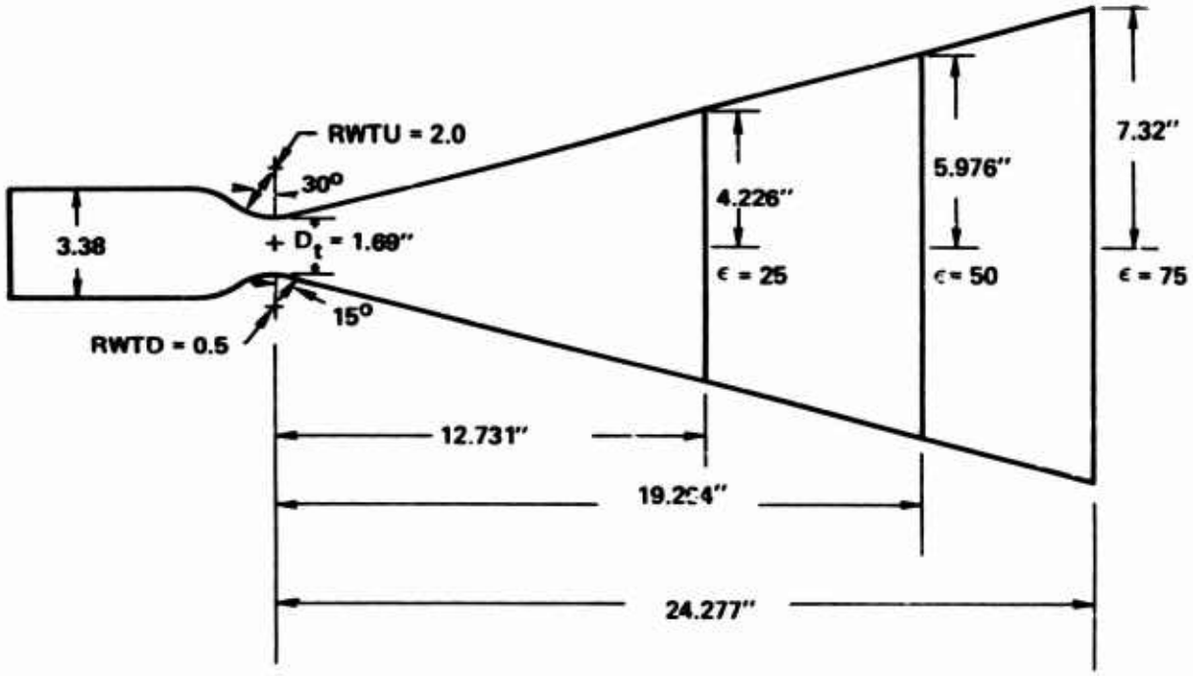

$(L/R)_1$ = 15.0631

$(L/R)_2$ = 22.7924

$(L/R)_3$ = 28.7235

Figure 1. 300# Thrust Engine (NTO/MMH)

TABLE 3

BELL NOZZLE CONTOURS IN SAME LENGTH AS
A 25/1, 15° CONICAL NOZZLE

80% Bell		75% Bell		70% Bell		65% Bell	
X/R_t	Y/R_t	X/R_t	Y/R_t	X/R_t	Y/R_t	X/R_t	Y/R_t
0.4574	1.1724	0.4894	1.1943	0.5283	1.2220	0.5825	1.2623
0.6603	1.2824	0.7153	1.3219	0.7835	1.3725	0.8802	1.4470
0.9009	1.4159	1.2891	1.6531	1.4360	1.7633	1.6469	1.9263
1.4726	1.7337	1.9910	2.0488	2.6898	2.4773	2.6019	2.4949
2.1432	2.0933	3.2456	2.7002	4.2397	3.2555	4.3547	3.4269
2.9012	2.4743	4.7337	3.3753	6.0731	4.0481	6.4801	4.3920
4.1999	3.0600	6.4478	4.0459	8.1842	4.8288	8.9681	5.3528
5.6860	3.6418	9.0770	4.9062	11.4186	5.8241	12.8357	6.5889
7.9520	4.3875	12.0877	5.7065	15.0631	6.7318	15.0631	7.1935
10.5343	5.0803	15.0631	6.3512	$\epsilon = 45.32$		$\epsilon = 51.75$	
12.6734	5.5571	$\epsilon = 40.34$		$\theta_E = 12.6°$		$\theta_E = 14.3°$	
15.0631	6.0072	$\theta_E = 11.1°$		$\theta_m = 27.42°$		$\theta_m = 28.62°$	
$\epsilon = 36.09$		$\theta_m = 26.43°$					
$\theta_E = 9.76°$							
$\theta_m = 25.52°$							

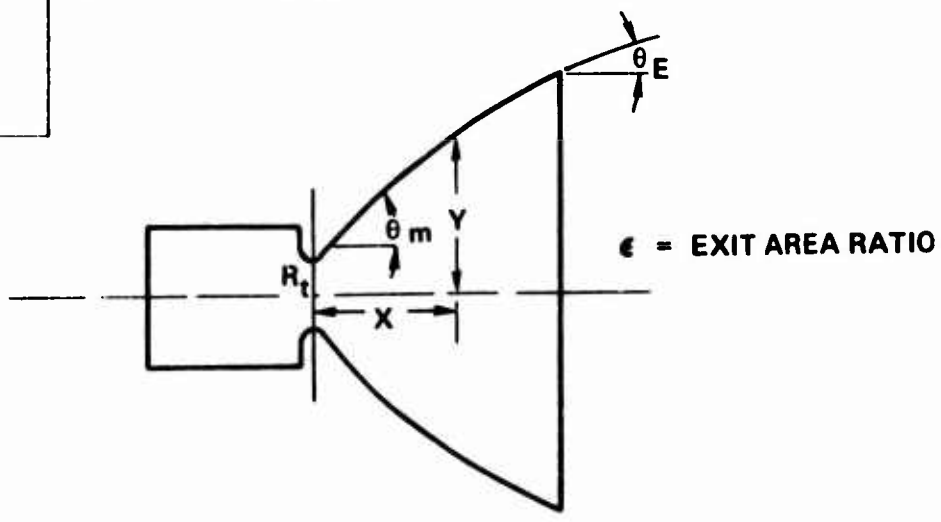

TABLE 4

BELL NOZZLE CONTOURS IN SAME LENGTH
AS A 50/1, 15° CONICAL NOZZLE

80% Bell		75% Bell		70% Bell	
X/R_t	Y/R_t	X/R_t	Y/R_t	X/R_t	Y/R_t
0.5605	1.2457	0.3679	1.1350	0.6568	1.3201
0.8408	1.4163	0.9194	1.4779	1.0159	1.5558
1.5601	1.8589	1.7349	1.9944	1.9508	2.1660
2.4522	2.3847	2.7522	2.6059	3.1338	2.8874
4.0793	3.2472	4.6331	3.6081	5.3445	4.0684
6.0439	4.1403	6.9233	4.6462	8.0643	5.2930
9.1704	5.3200	10.5966	6.0193	12.4591	6.9159
12.8621	6.4456	14.9585	7.3317	17.7122	8.4701
17.1037	7.4882	18.6708	8.2553	22.7924	9.6949
22.7924	8.5841	22.7924	9.1150	$\epsilon = 93.99$	
$\epsilon = 73.69$		$\epsilon = 83.08$		$\theta_E = 12.4^\circ$	
$\theta_E = 9.55^\circ$		$\theta_E = 10.95^\circ$		$\theta_m = 30^\circ$	
$\theta_m = 28.15^\circ$		$\theta_m = 29.05^\circ$			

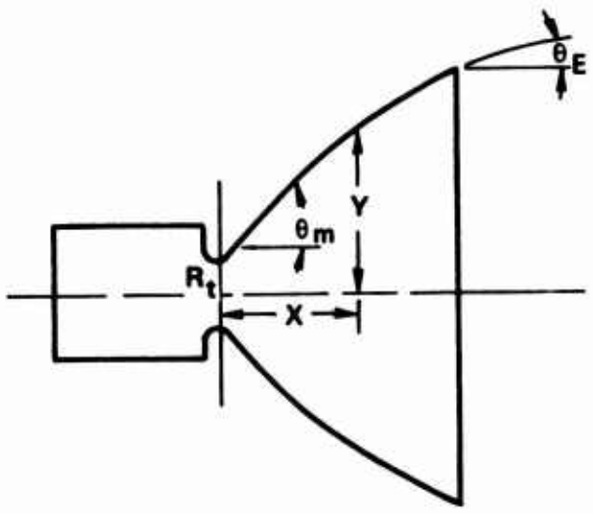

SECTION III

MODEL INPUT

The TDK computer code requires input data in basically four categories. The first two include the engine's geometrical configuration and operating conditions. They have been discussed in the previous Section. The last two categories are the chemical bipropellant used and the subsequent chemical reactions which take place in the engine.

1. Propellant Considered

The storable bipropellant used for this study was NTO/MMH. This combination was chosen because of its possible use in future engine systems such as in upgraded Agena or the Space Tug. Further, this combination is one level higher on the performance scale than most current operating systems that employ a liquid storable bipropellant. The propellant specifics are as follows:

NITROGEN TETROXIDE

Chemical Formula: $N_{2.1822}O_{4.3396}H_{0.0111}$

Heat of Formation @ 298.15°F (Cal/mole): -5.481

Molecular Weight: 100

MONOMETHYLHYDRAZINE . 'H

Chemical Formula: $CH_3N_2H_3$

Heat of Formation @ 298.15°F (Cal/mole): 13,104

Molecular Weight: 46.075

2. Chemical Reactions

The basic phenomenological relationship describing chemical reaction rates is provided by the law of mass action (Reference 8). This law forms the relationship between the rate of production of a chemical species and its concentration (Mj) and stoichiometric coefficient (ν_j).

This can be expressed as

$$\text{Rate of reaction} = K_f \prod_{j=1}^{n} (M_j)^{j'} \tag{5}$$

where the forward reaction rate constant K_f depends only on the temperature. The reaction rate constant is an empirically determined coefficient and has the form

$$K_f = B\, T^x \exp(-E/RT). \tag{6}$$

The frequency factor B, the exponential x, and the activation energy E are all unique to the specific reaction being considered. Table 5 lists the twenty-four reactions considered for this propellant system and the appropriate coefficients which were used to define their chemical interaction. The values given in columns two, three and four of Table 5 were taken from Reference 6

TABLE 5

REACTION RATE DATA

Reactions	Reaction Rate Parameter B $\frac{cm^6\text{-}^oK^\alpha}{mole^2\text{-}sec}$	Reaction Rate Parameter E (K_{cal}/mol)	α
Third Body Reactions			
$CO + O + M = CO_2 + M$	0.1×10^{17}	3.5	0.0
$OH + H + M = H_2O + M$	0.1×10^{20}	0.0	1.0
$C + O + M = CO + M$	0.3×10^{17}	0.0	0.5
$H + H + M = H_2 + M$	0.75×10^{19}	0.0	1.0
$N + N + M = N_2 + M$	0.10×10^{19}	0.0	1.0
$N + O + M = NO + M$	0.60×10^{17}	0.0	0.5
$O + H + M = OH + M$	0.20×10^{19}	0.0	1.0
$O + O + M = O_2 + M$	0.19×10^{17}	0.0	0.5
Binary Exchange Reactions	B $\frac{cm^3\text{-}K^\alpha}{mole\text{-}sec}$	E (kal/mole)	α
$OH + CO = CO_2 + H$	0.31×10^{12}	0.6	0.0
$O2 + CO = CO_2 + O$	0.35×10^{13}	51.0	0.0
$H_2 + OH = H_2O + H$	0.60×10^{12}	5.0	-0.5
$OH + OH = H_2O + O$	0.10666×10^{14}	0.96671	0.0134
$CO_2 + C = CO + CO$	0.105×10^{12}	6.9949	-0.5
$OH + C = CO + H$	0.53×10^{12}	5.6278	-0.5
$NO + C = CO + N$	0.53×10^{12}	8.3025	-0.5
$CO_2 + N = NO + CO$	0.105×10^{12}	59.616	-0.5
$O_2 + C = CO + O$	0.53×10^{12}	6.5518	-0.5
$OH + H = H_2 + O$	0.14×10^{13}	5.19	0.0
$OH + OH = H_2 + O_2$	0.14127×10^{14}	49.2644	0.015
$NO + N = N_2 + O$	0.15×10^{14}	0.0	0.0
$NO + NO = N_2 + O_2$	0.10×10^{14}	79.488	0.0
$OH + N = NO + H$	0.53×10^{12}	5.6278	-0.5
$O_2 + N = NO + O$	0.18×10^{9}	6.001	-1.5
$OH + O = O_2 + H$	0.32×10^{12}	0.10	-4.7

SECTION IV

RESULTS

The results from Study 1, which are summarized in Figures 2-13 and Tables 6 and 7, reveal a number of interesting observations.

1. Mixture Ratio Effects

First, the greatest performance loss due to kinetics for the 15° conical nozzle occurs at a mixture ratio of 2.5, the maximum temperature condition. This condition occurs because at this point the maximum energy is available for dissociating the gaseous moelcules and radicals. Important as well are the specific reactions that take place and the energy it takes to dissociate the constituents in those reactions. Second, there is a definite slope change in the kinetic loss curves as one goes from a fuel to an oxidizer rich condition. This is caused by a change in the primary reaction mechanism as the mixture ratio increases past the stoichiometric point.

2. Chamber Pressure Effects

As can be seen in Figures 2-13, the magnitude of kinetic loss decreases as the chamber pressure increases. The primary cause of this relationship is the decrease in gas residence time with increased chamber pressure. Though this gives less time for recombination, the amount dissociated initially is dramatically decreased.

3. Engine Thrust Effects

Another parameter which has a significant impact on kinetic performance is engine thrust; the kinetics loss decreases with increased thrust. This decrease can be attributed to small nozzle area ratio gradients dA/dx in the higher thrust engines. The gas travels farther in a high thrust engine to reach the same area ratio than it does in a lower thrust, geometrically similar engine. This distance increase can be converted into a time increment or an increase in specie recombination time before the

flow is essentially chemically frozen. The net result is greater performance for the higher thrust engine.

4. Area Ratio Effects

Increasing the area ratio from 25 to 100 also affects the magnitude of the kinetic performance of a nozzle. The results shown in Tables 6 and 7 show that kinetics loss increases with a corresponding increase in area ratio. This would be expected since nozzle recombination takes place most rapidly at the near throat region, decreasing quite rapidly as the area ratio increases. Since recombination does take place throughout the nozzle, but at a decreasing rate, nozzle kinetics losses will increase area ratio.

5. Radius of Curvature Effects

The primary purpose of Study 2 was to vary the downstream normalized radius of curvature of a 150/1 area ratio conical nozzle and determine if a kinetic gain could be realized. The results summarized in Tables 8 and 9 and Figures 14 and 15 illustrate some of these data. These results seem to indicate that varying the radius of curvature has little potential in reducing the kinetics loss for the conditions considered. This is true for one basic reason. The increased nozzle length required to achieve the kinetics gain causes a correspondingly higher weight penalty and thus an overall performance loss. For this propellant combination at any of the operating conditions used, a radius of curvature as small as possible should be used to minimize nozzle length or maximize nozzle area ratio for the given length.

6. Bell Nozzle Kinetics Losses

The third study used a number of Bell type contours which had the same axial lengths as both a 25/1 and 50/1 conical nozzle. The results are interesting because the overall performance is much greater than that of a 15^{o} conical nozzle, but the kinetic losses incurred by unrecombined species are also larger. An example of this is illustrated in Figure 16; other Bell nozzle data are summarized in Table 10. From these data we find that a

15^{o} cone is kinetically much more efficient than a typical Bell nozzle but lacks the overall higher performance of the Bell. A worthwhile endeavor would be to try to achieve the same kinetic efficiency in a Bell nozzle as is present in the 15^{o} conical nozzle, thereby increasing the overall specific impulse of a Bell nozzle by 6 seconds. This could be done, for example, by changing the Bell nozzle contour in the near throat region but still expanding the gases to the higher Bell area ratio.

SECTION V

CONCLUSIONS

A number of conclusions can be reached from the data presented:

(1) As shown in Figure 2 kinetics losses can be as large as 20 seconds Isp with NOT/MMH at certain operating conditions, such as low thrust, low chamber pressure, and stoichiometric mixture ratio.

(2) The following variables, listed in decreasing order of influence, affect kinetic losses: MR, P_c, ε, THRUST, and R_c.

(3) Kinetics losses reach a maximum at the stoichiometric point.

(4) Kinetics losses decrease with increasing chamber pressure.

(5) Kinetics losses increase with increasing area ratio.

(6) Kinetics losses decrease with increasing throat size.

(7) Kinetics losses decrease with increased downstream radius of curvature.

Other efforts that would have added immeasurably to this study but could not be undertaken due to lack of time:

(1) Obtain a correlation function for determining the kinetics losses of engines for which the range of variables considered in this study apply.

(2) Determine the point at which the gas flow is essentially chemically frozen for the variables considered in this study.

(3) Determine the primary chemical reactions which take place as mixture ratio is varied.

(4) Construct a Bell contour that will have essentially the same kinetic efficiency as a 15° cone but also increase overall performance by maintaining other performance levels.

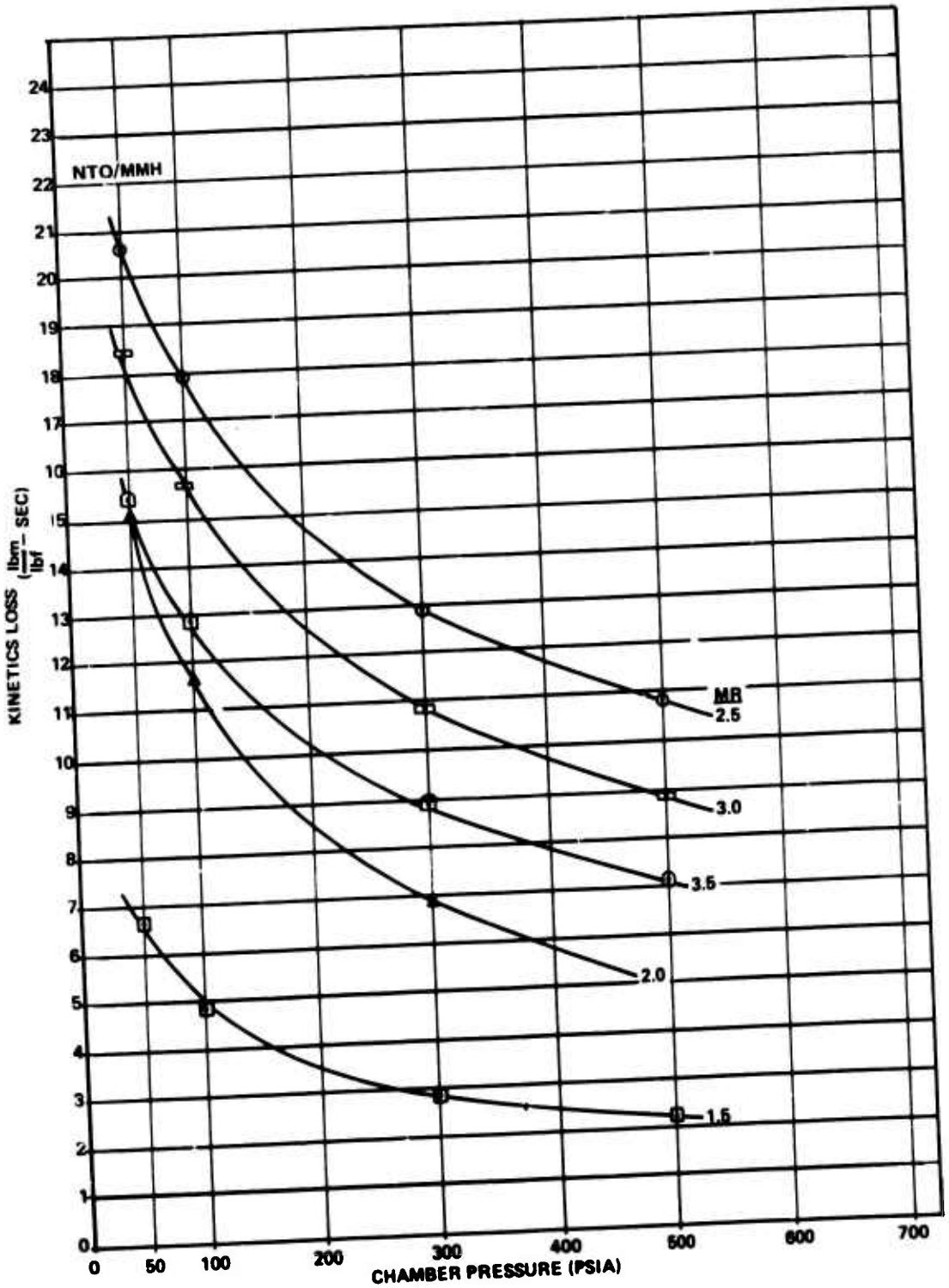

Figure 2. Kinetics Loss of a 25/1, 15° Conical Nozzle Operating at 300# Thrust

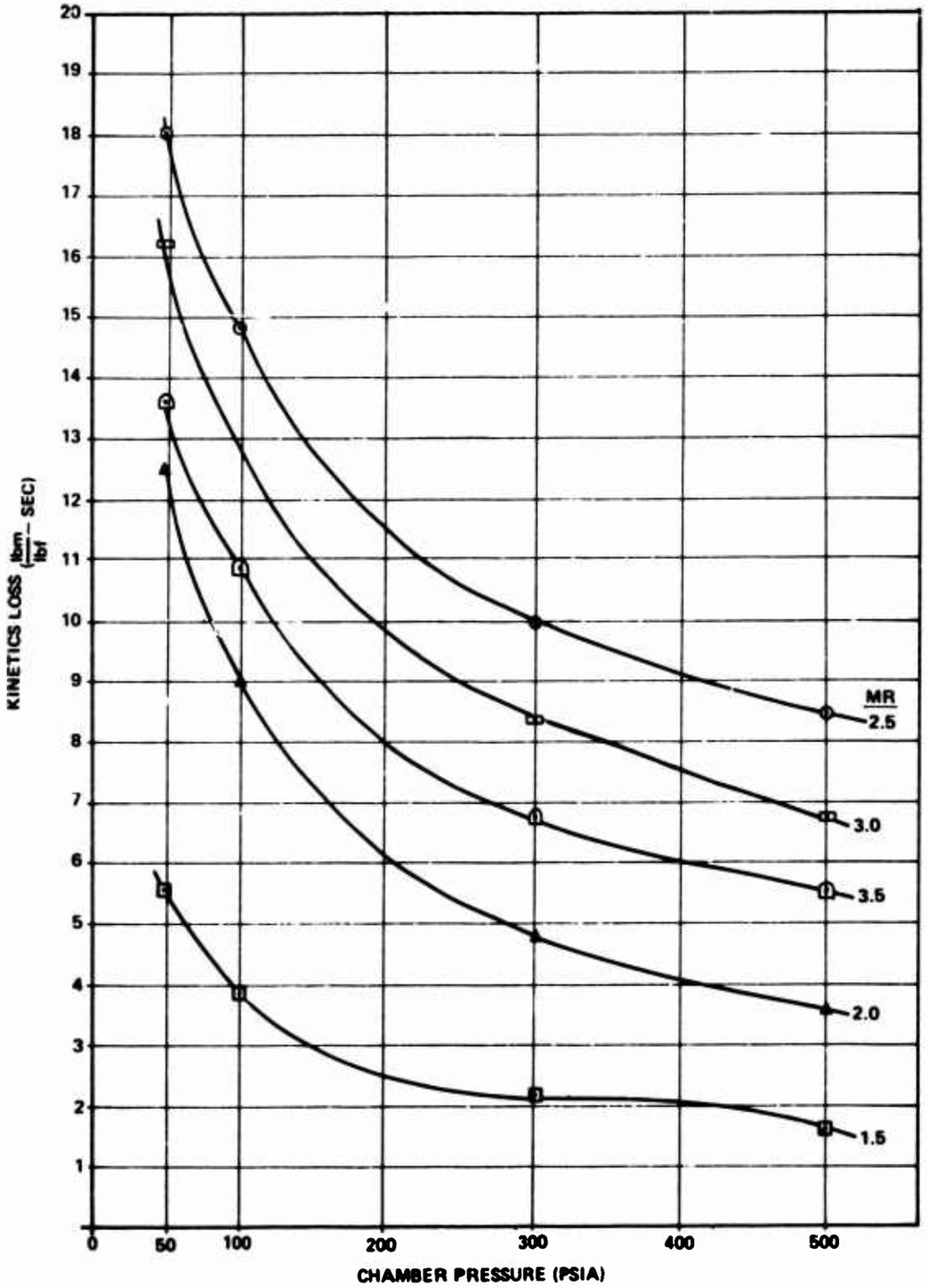

Figure 3. Kinetics Loss of a 25/1, 15° Conical Nozzle Operating at 3000# Thrust

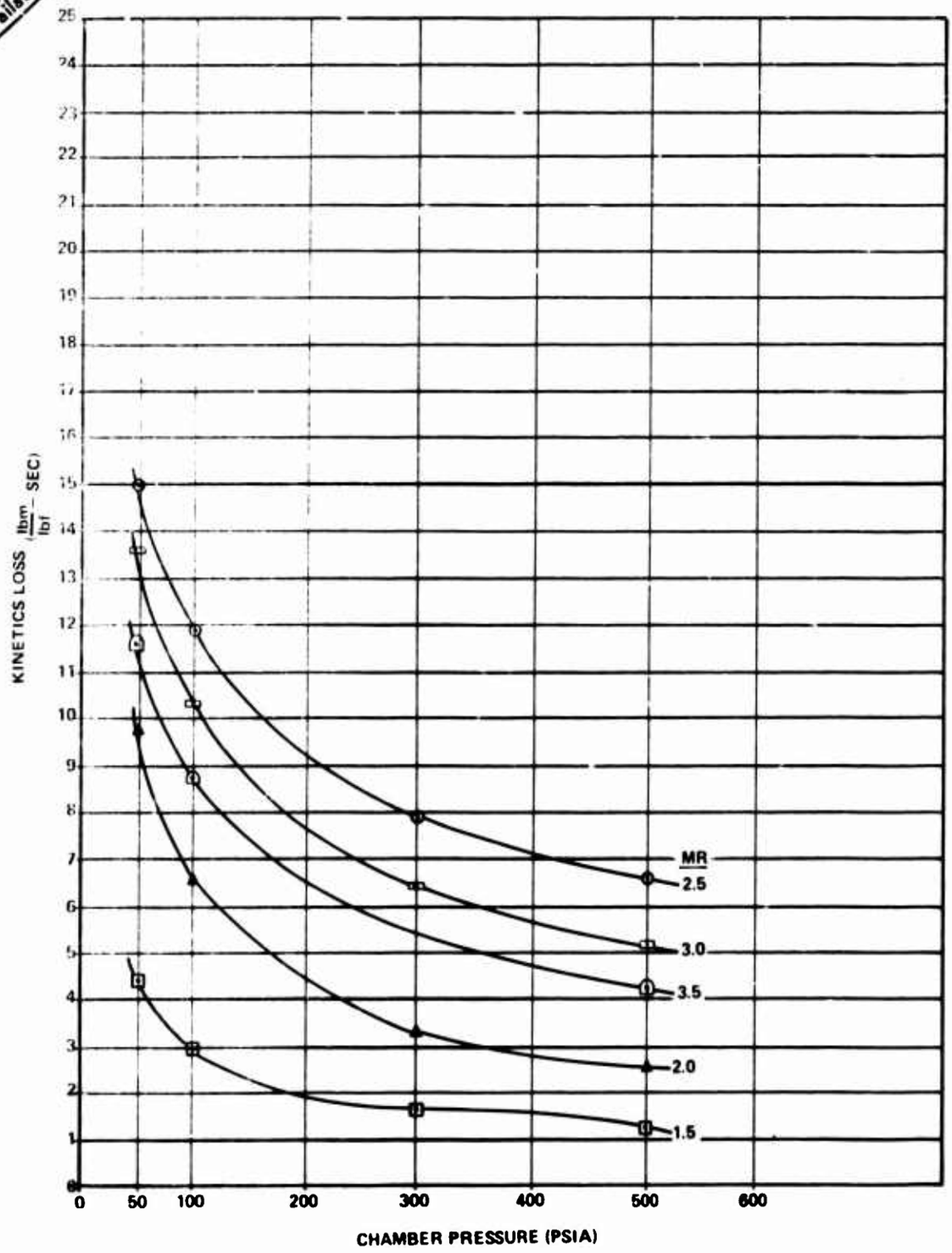

Figure 4. Kinetics Loss of a 25/1, 15° Conical Nozzle Operating at 18000# Thrust

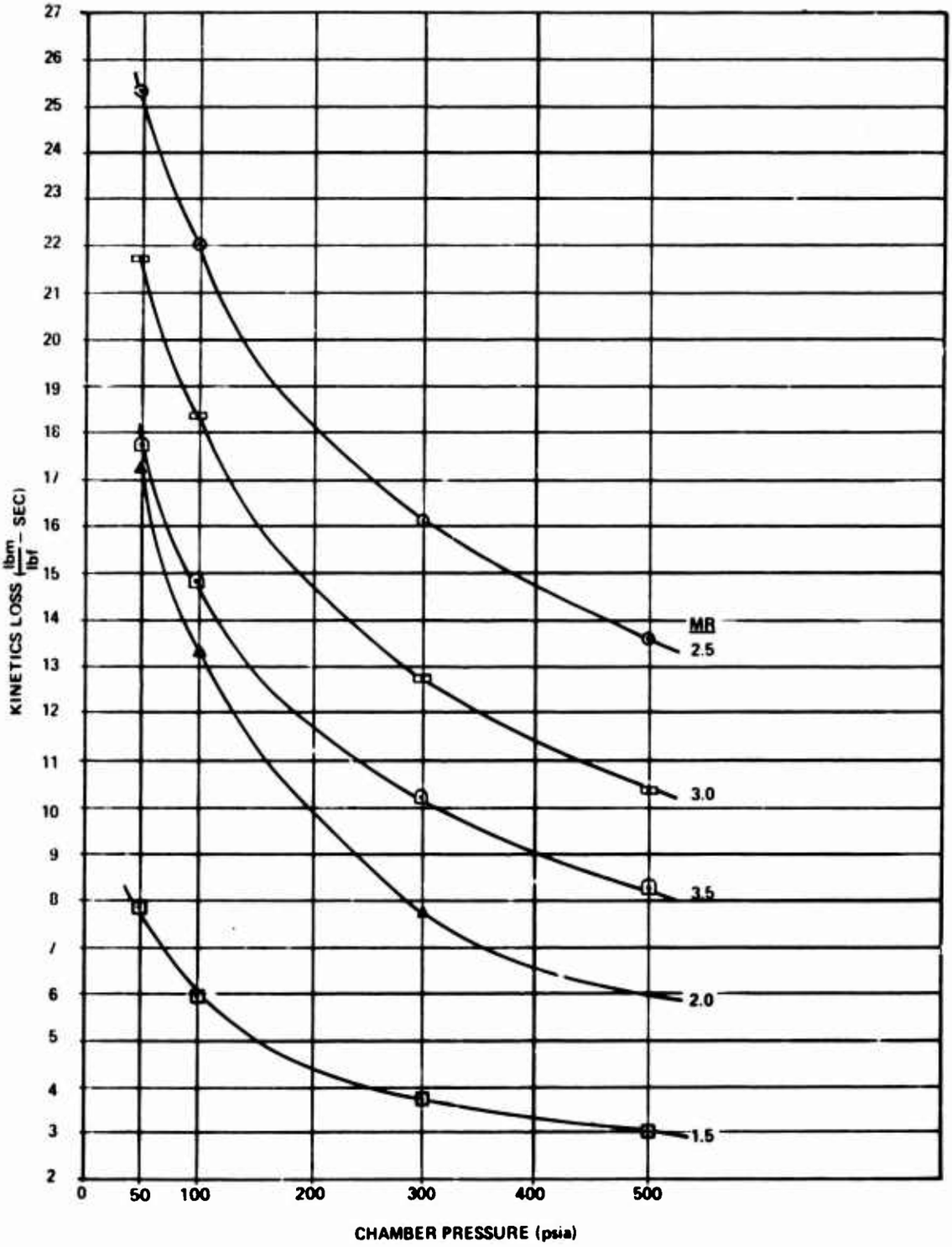

Figure 5. Kinetics Loss of a 50/1, 15° Conical Nozzle Operating at 300# Thrust

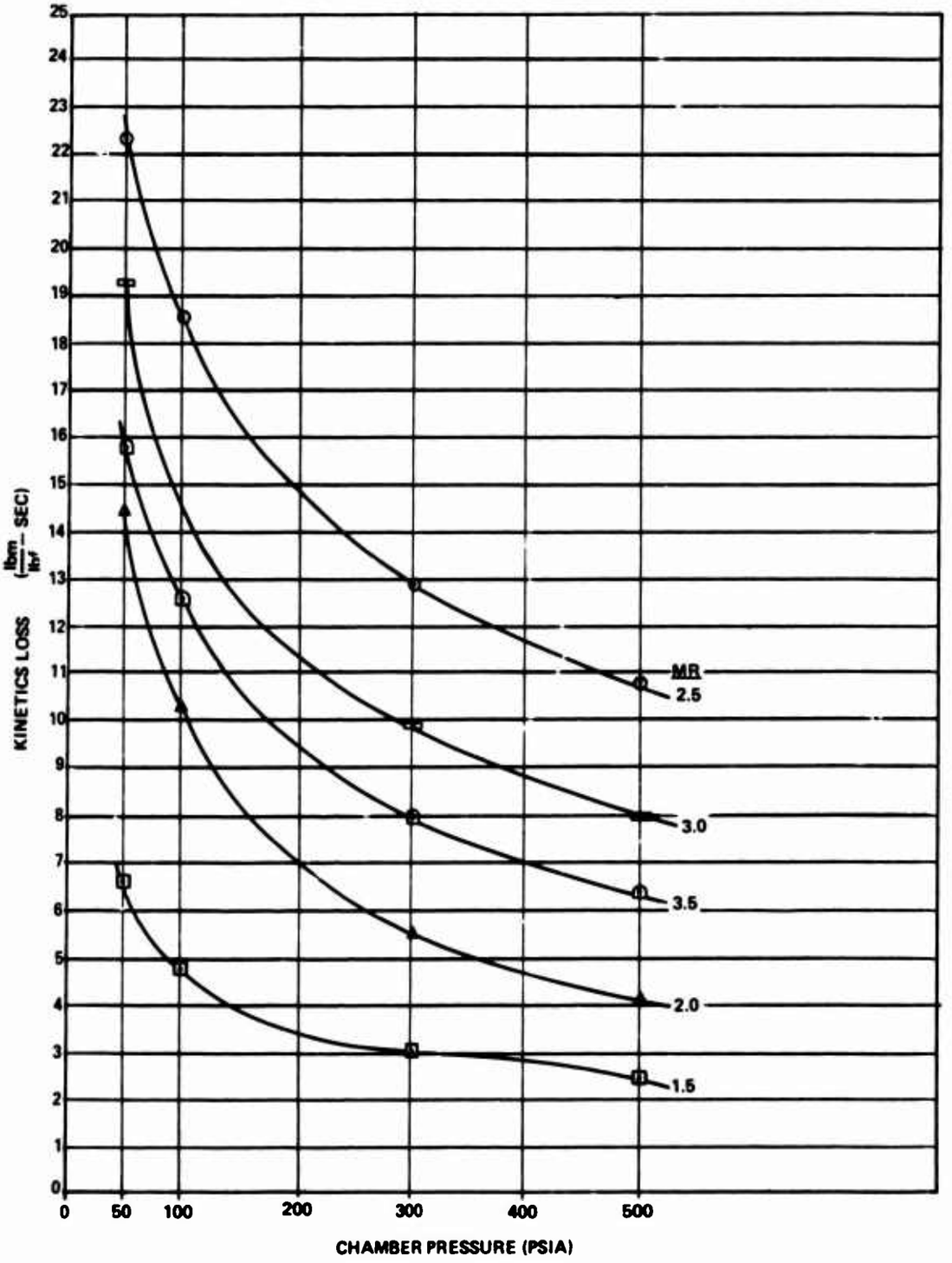

Figure 6. Kinetics Loss of a 50/1, 15° Conical Nozzle Operating at 3000# Thrust

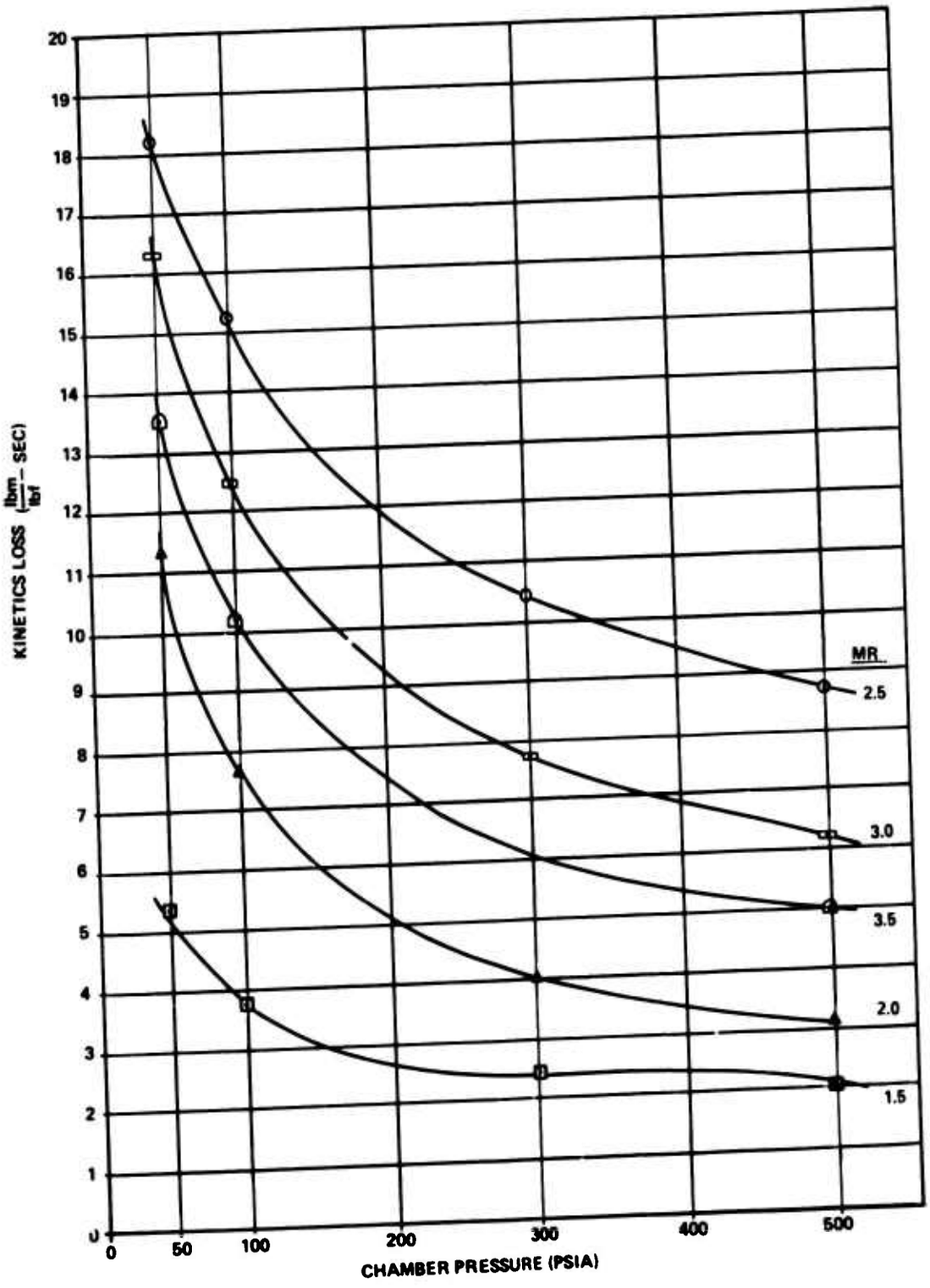

Figure 7. Kinetics Loss of a 50/1, 15° Conical Nozzle Operating at 18000# Thrust

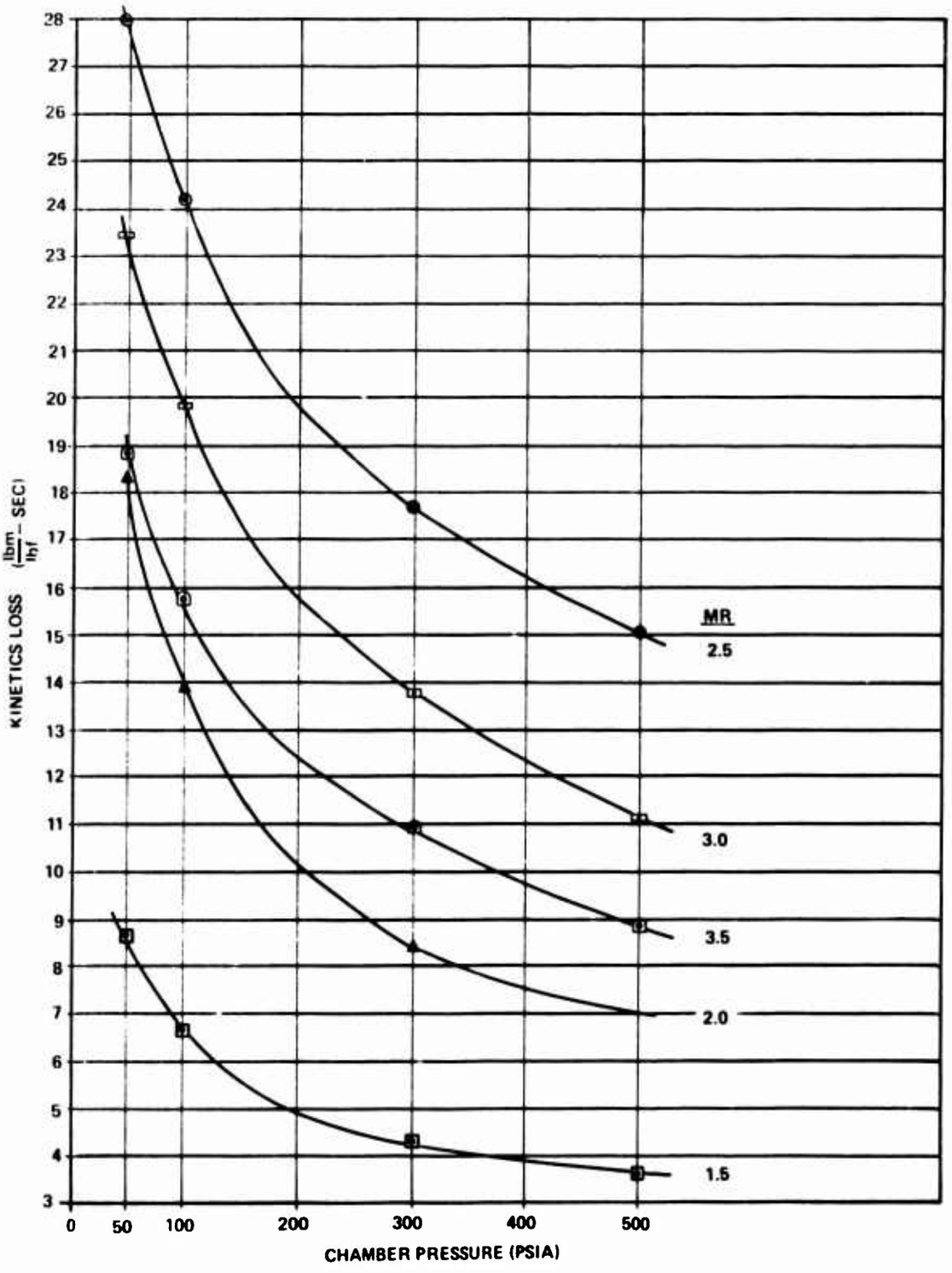

Figure 8. Kinetics Loss of a 75/1, 15° Conical Nozzle Operating at 300# Thrust

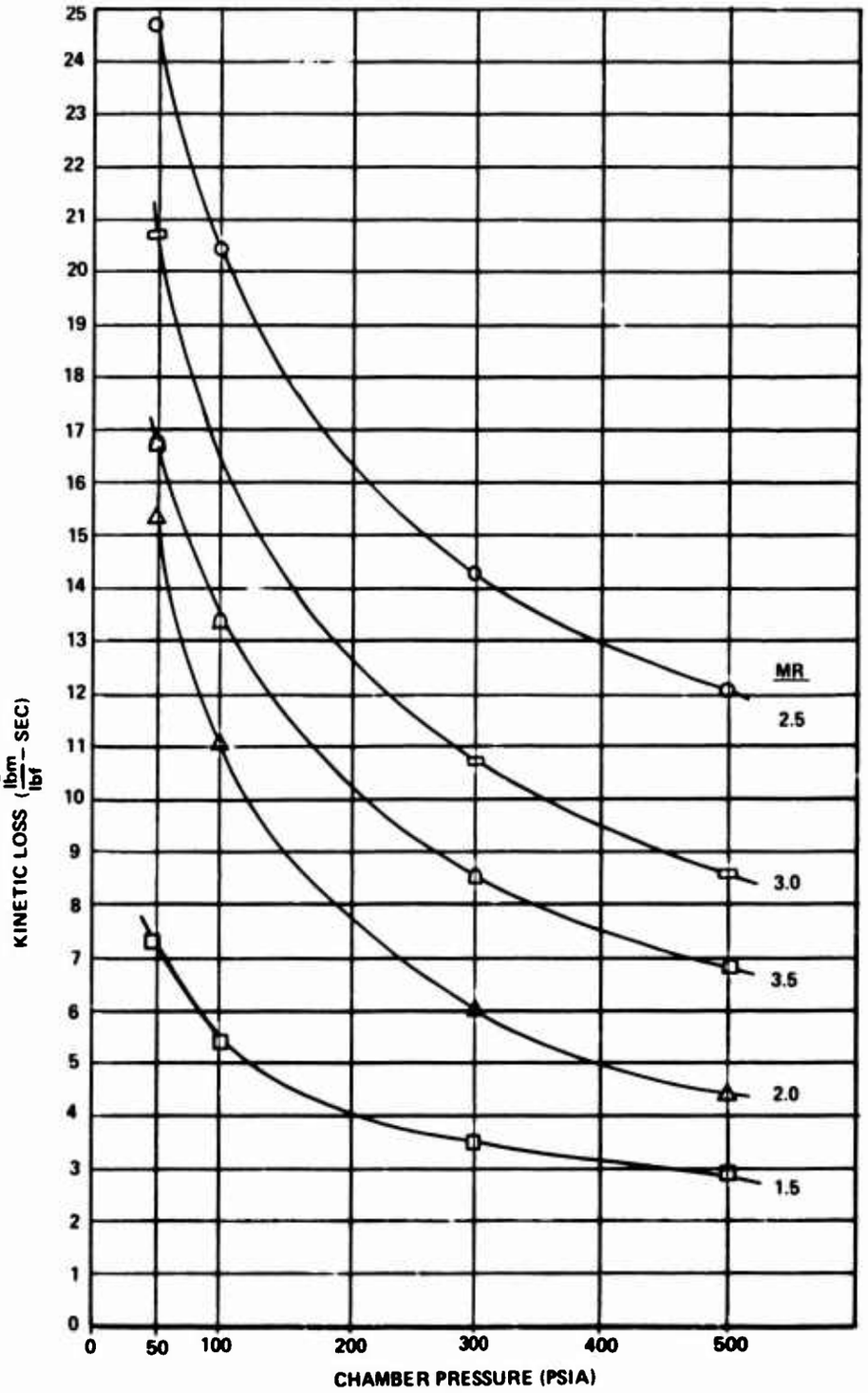

Figure 9. Kinetics Loss of a 75/1, 15° Conical Nozzle Operating at 3000# Thrust

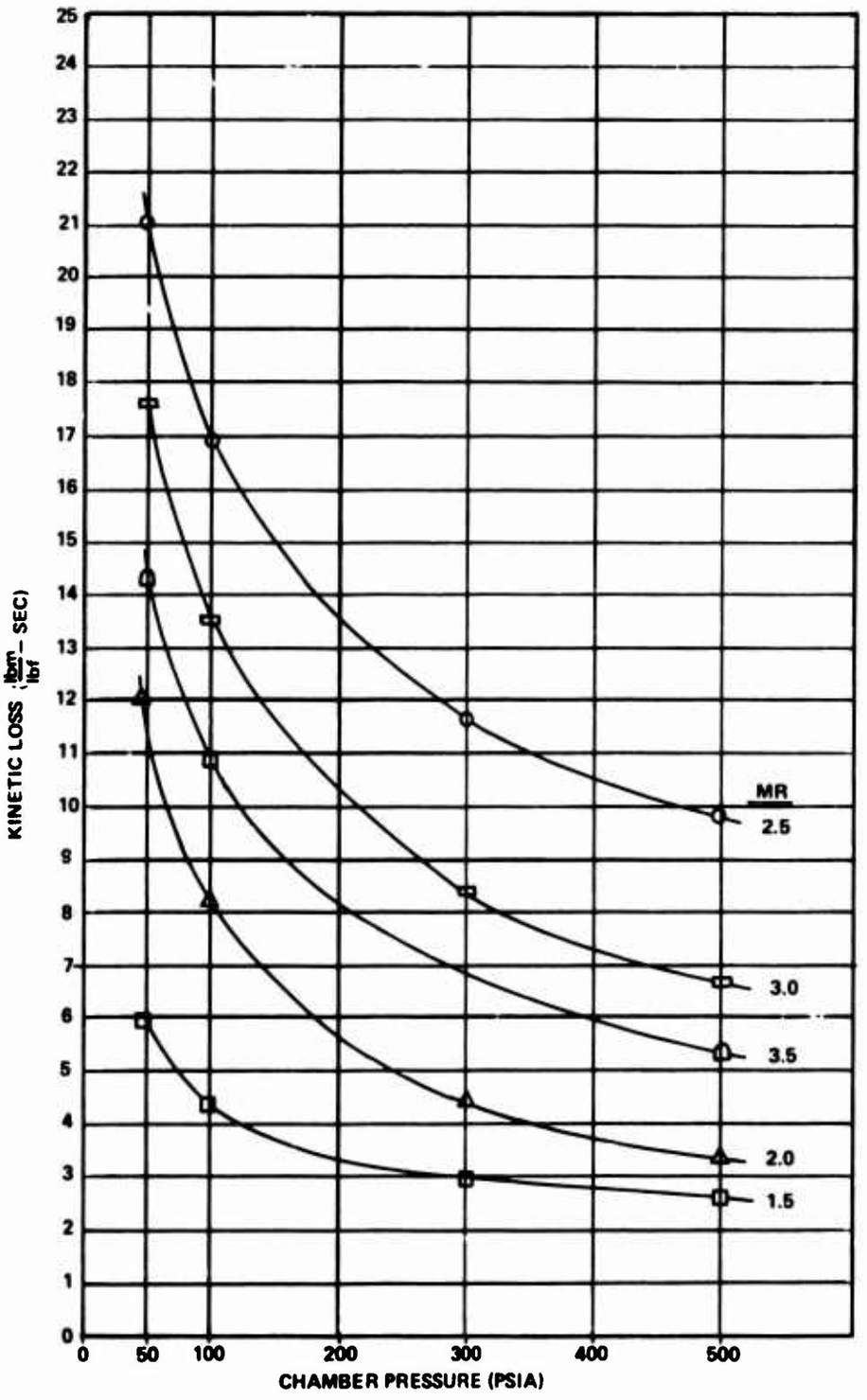

Figure 10. Kinetics Loss of a 75/1, 15° Conical Nozzle Operating at 18000# Thrust

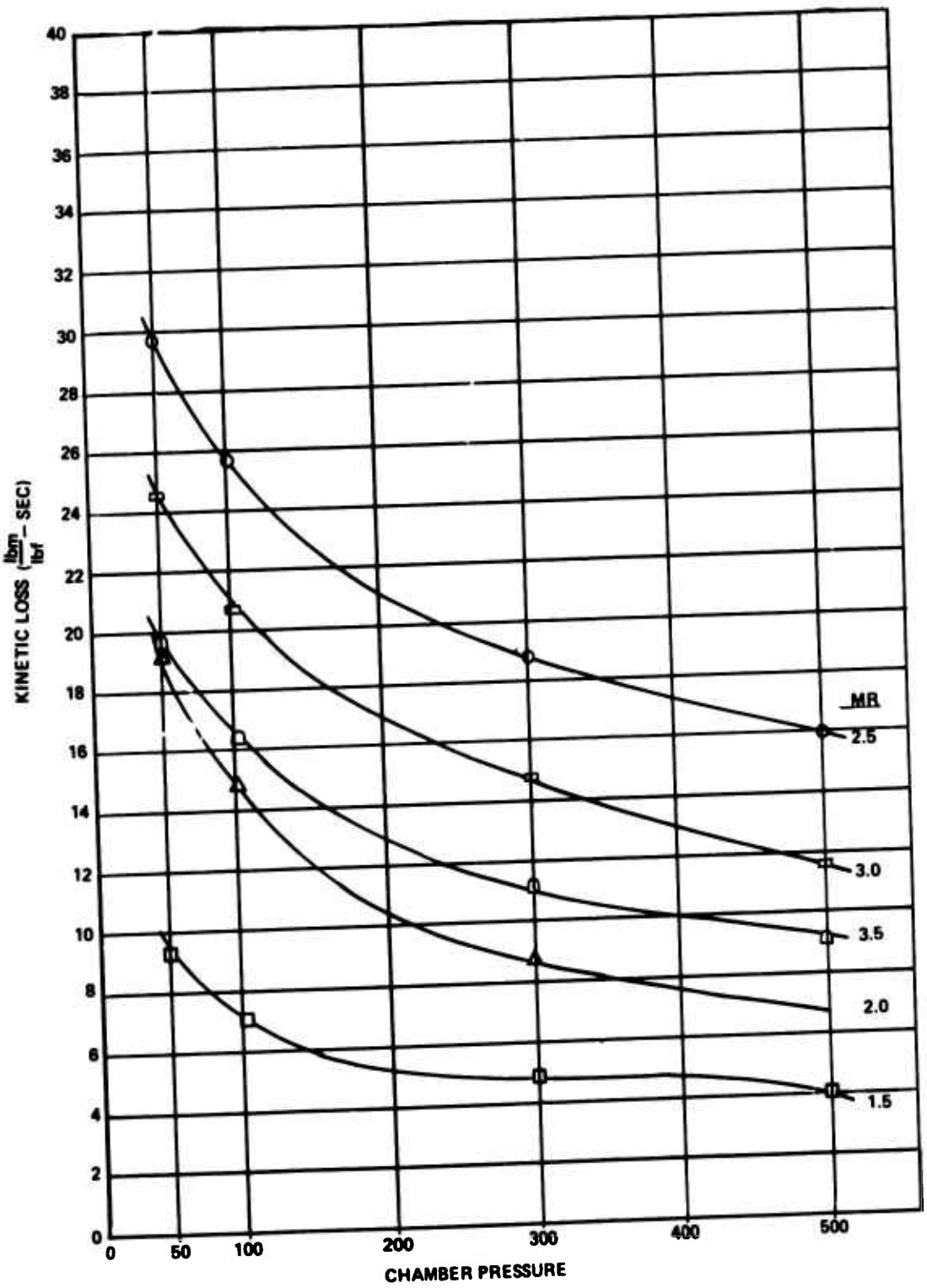

Figure 11. Kinetics Loss of a 100/1, 15° Conical Nozzle Operating at 200# Thrust

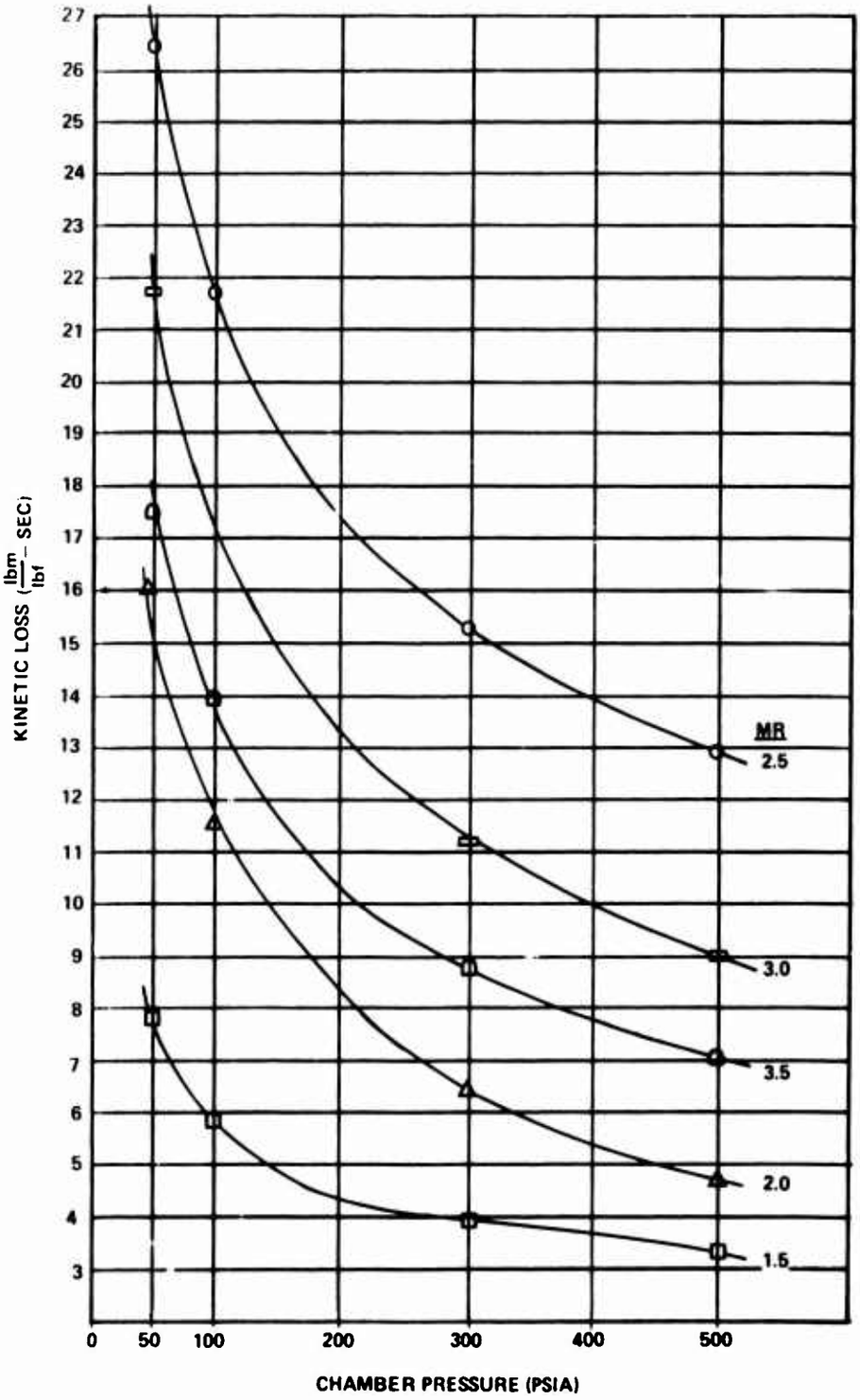

Figure 12. Kinetics Loss of a 100/1, 15° Conical Nozzle Operating at 3000# Thrust

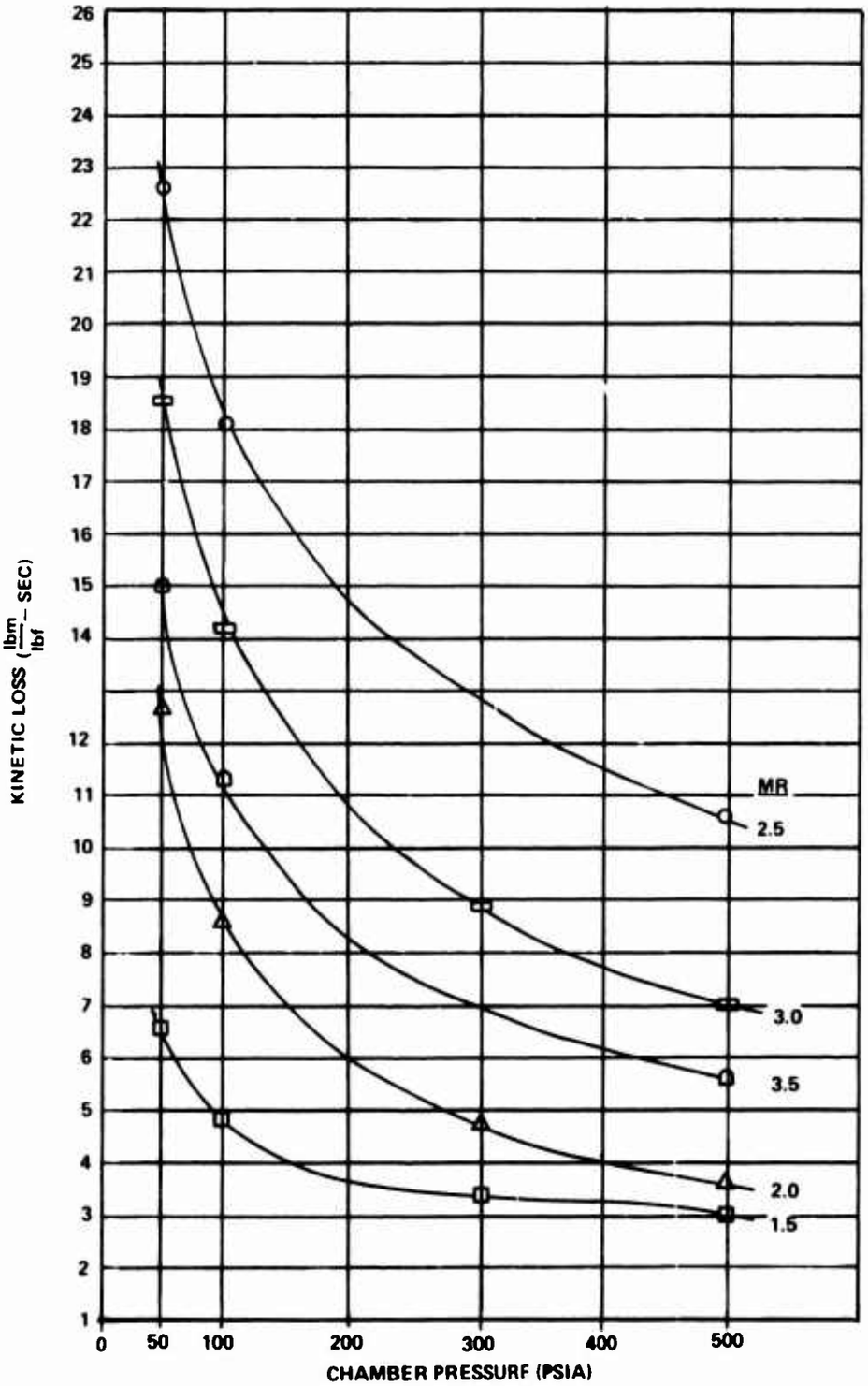

Figure 13. Kinetics Loss of a 100/1, 15° Conical Nozzle Operating at 18000# Thrust

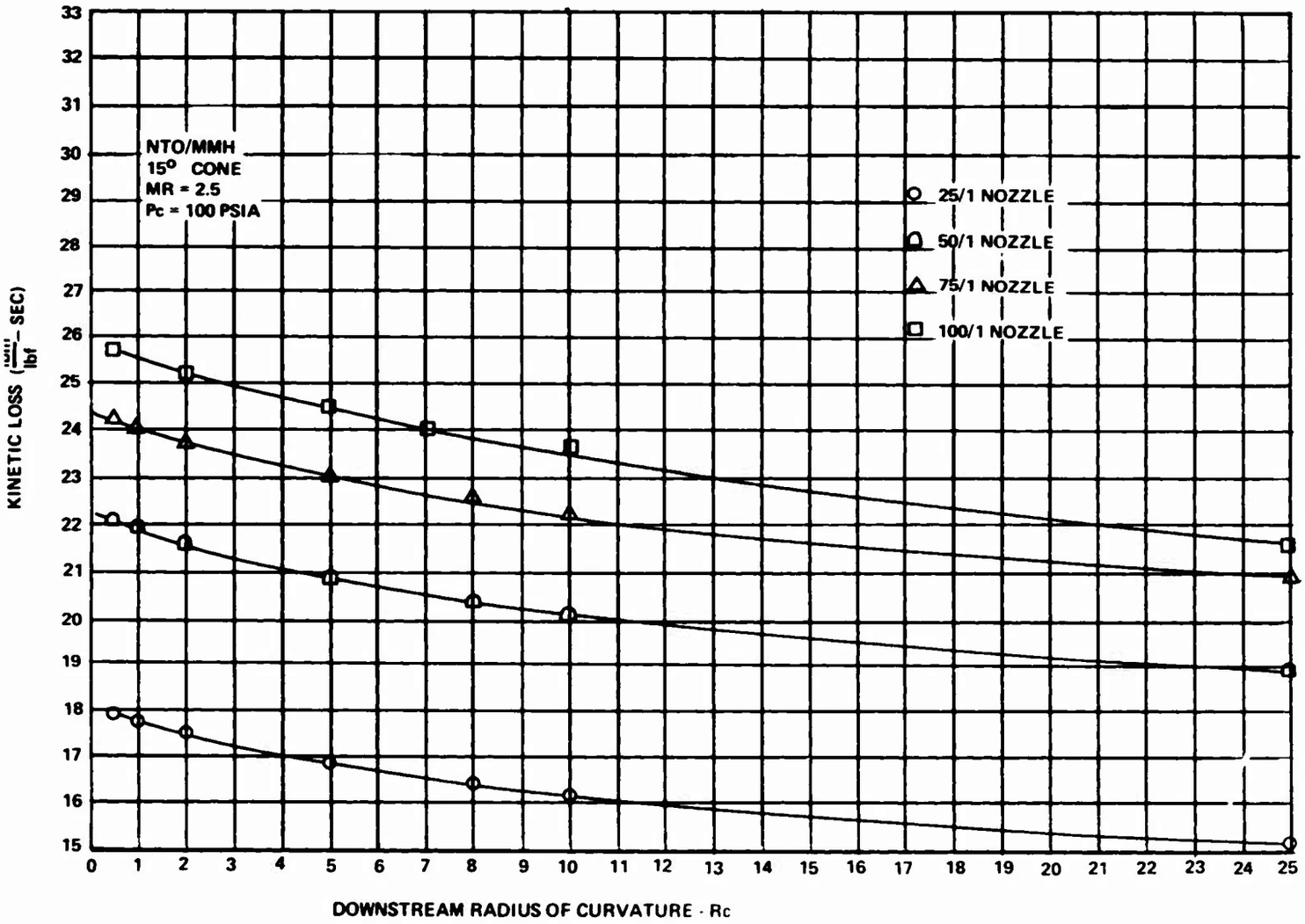

Figure 14. Influence of Radius of Curvature on Kinetics Loss at 300# Thrust

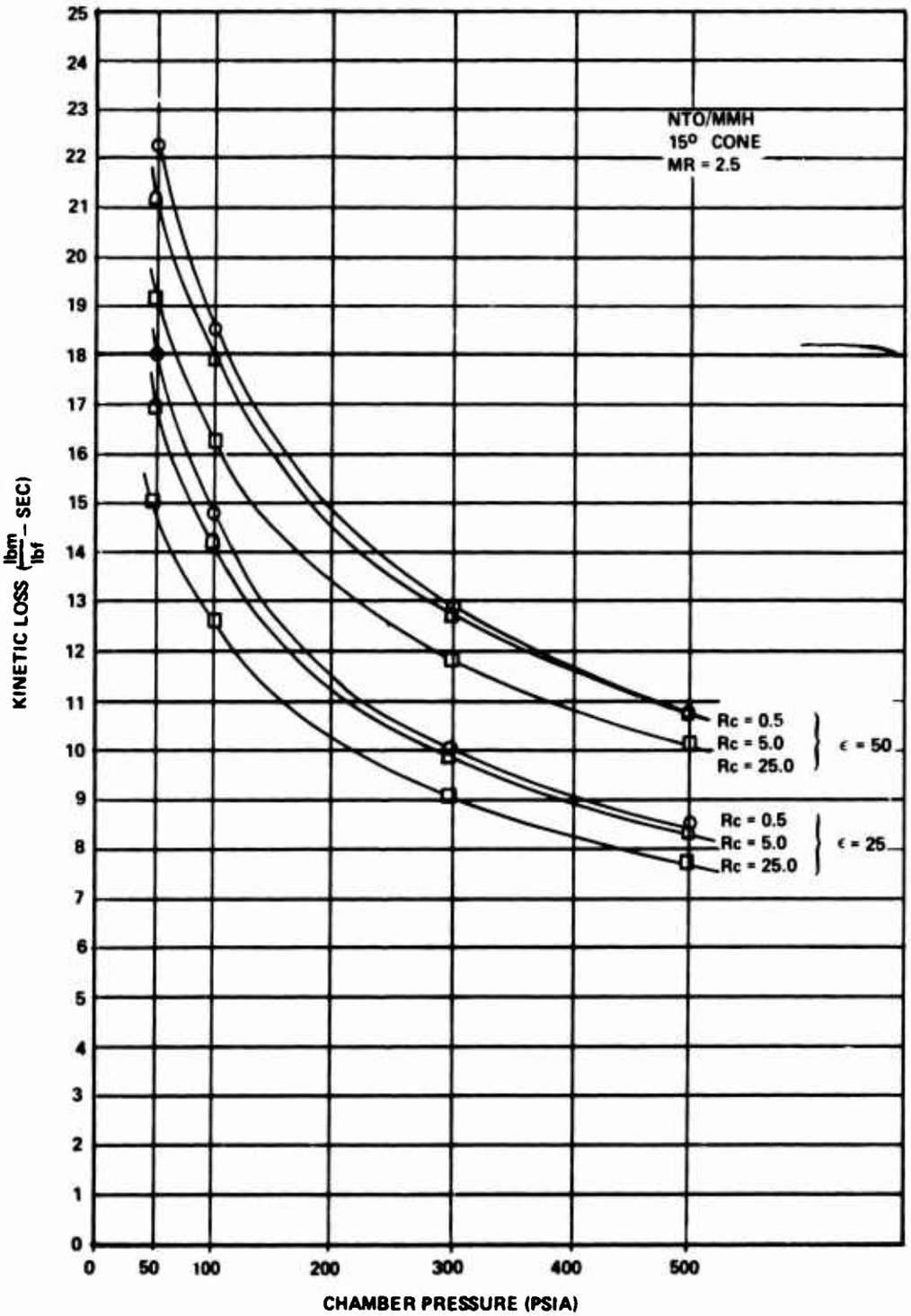

Figure 15. Influence of Nozzle Geometry on Kinetic Performance at 3000# Thrust

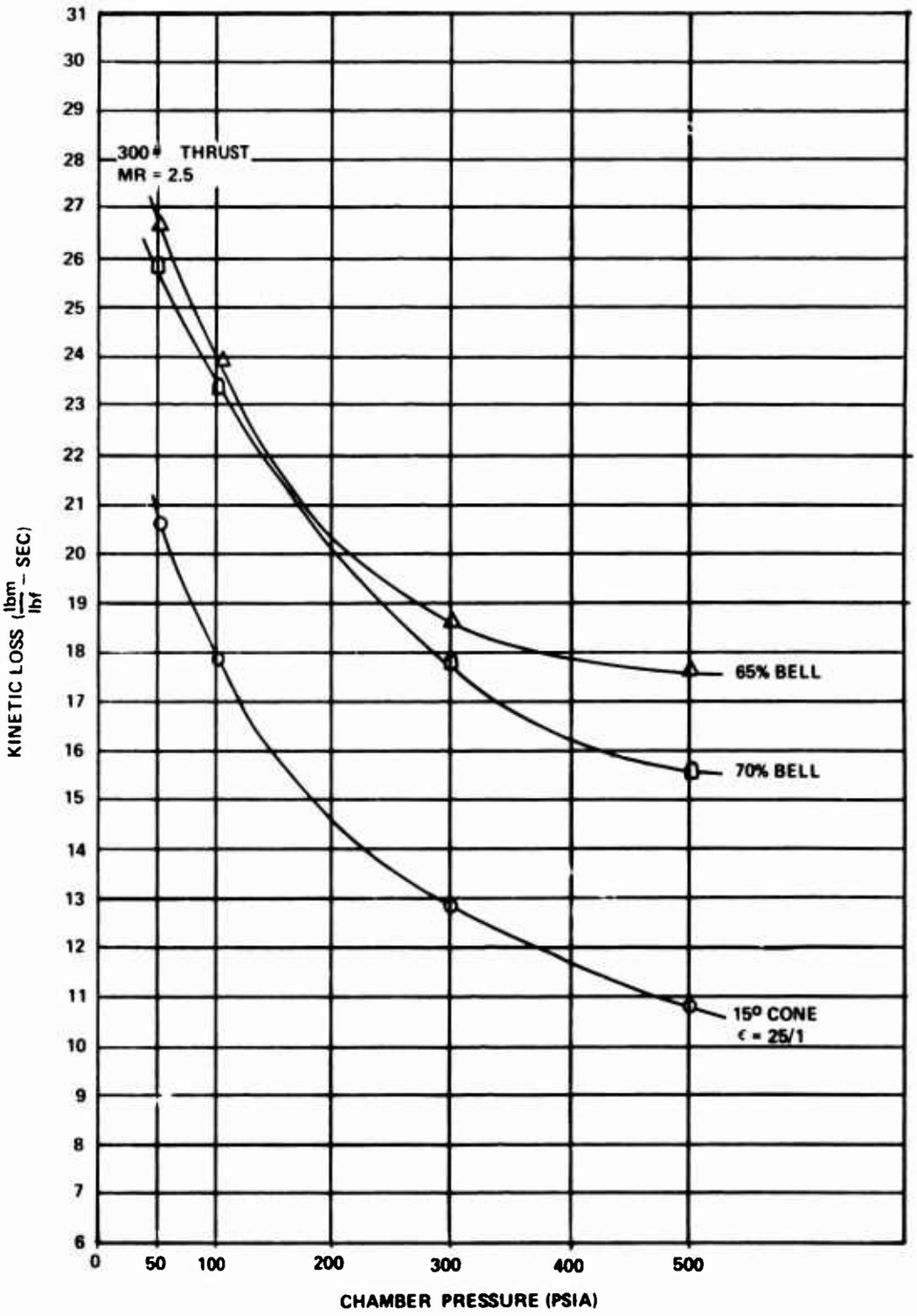

Figure 16. Kinetics Loss Comparisons Between 15° Cone and Various Bell Nozzles

TABLE 6

KINETICS LOSS SUMMARY OF 15° CONE (Part 1)

Thrust (lbf)	300#				3000#				18000#			
P_c (psia) / MR	50	100	300	500	50	100	300	500	50	100	300	500
ε = 25												
1.5	6.64	4.84	2.825	2.21	5.53	3.81	2.15	1.56	4.41	2.91	1.69	1.29
2.0	15.01	11.68	6.768		12.52	8.98	4.75	3.53	9.81	6.61	3.36	2.61
2.5	20.63	17.9	12.9	10.81	18.0	14.80	9.97	8.40	14.99	11.90	7.92	6.60
3.0	18.39	15.66	10.84	8.80	16.19	13.04	8.30	6.69	13.59	10.34	6.43	5.16
3.5	15.27	12.84	8.85	7.130	13.57	10.83	6.72	5.44	11.54	8.71		4.22
ε = 50												
1.5	7.85	5.908	3.741	3.09	6.60	4.75	2.99	2.38	5.344	3.75	2.48	2.09
2.0	17.22	13.35	7.788		14.38	10.30	5.53	4.14	11.32	7.64	4.05	3.11
2.5	25.34	22.03	16.1	13.54	22.33	18.51	12.85	10.78	18.20	15.21	10.40	8.69
3.0	21.71	18.353	12.71	10.35	19.20	15.38	9.84	7.97	16.27	12.45	7.72	6.21
3.5	17.67	14.78	10.198	8.22	15.74	12.51	7.93	6.33	13.54	10.14		4.97

TABLE 7

KINETICS LOSS SUMMARY OF 15° CONE (Part 2)

Thrust (lbf)	300#				3000#				18000#			
P_c (psia) / MR	50	100	300	500	50	100	300	500	50	100	300	500
ε = 75												
1.5	8.64	6.593	4.278	3.60	7.32	5.40	3.49	2.88	5.99	4.35	2.95	2.56
2.0	18.32	13.93	8.362		15.30	11.03	5.98	4.46	12.05	8.22	4.42	3.37
2.5	27.92	24.2	17.73	15.03	24.7	20.45	14.27	12.08	21.07	16.94	11.65	9.83
3.0	23.44	19.799	13.77	11.09	20.76	16.64	10.73	8.56	17.64	13.53	8.37	6.69
3.5	18.78	15.75	10.85	8.80	16.73	13.35	8.46	6.80	14.29	10.83		5.36
ε = 100												
1.5	9.20	7.114	4.748	4.06	7.84	5.88	3.94	3.32	6.47	4.79	3.38	2.99
2.0	19.16	14.90	8.822		16.02	11.54	6.36	4.71	12.65	8.62	4.74	3.58
2.5	29.73	25.67	18.88	15.98	26.39	21.77	15.28	12.91	22.60	18.12		10.56
3.0	24.55	20.689	14.37	11.61	21.76	17.41	11.22	8.98	18.52	14.18	8.86	7.03
3.5	19.61	16.39	11.25	9.13	17.47	13.89	8.77	7.06	14.94	11.29		5.57

TABLE 8

KINETICS LOSS - RADIUS OF CURVATURE STUDY (Part 1)

	300#				3000#				18000#			
PC / Rad of Curv	50	100	300	500	50	100	300	500	50	100	300	500
ε = 25												
1.0		17.75										
2.0		17.49										
3.0						14.40				11.81		
5.0	19.59	16.85	12.39	10.73	16.91	14.20	9.93	8.34	14.41	11.70	7.88	6.54
8.0		16.39				13.85				11.51		
10.0		16.13				13.65				11.39		
25.0	17.59	15.00	11.11	9.59	15.05	12.67	9.07	7.73	12.84	10.61	7.35	6.18
ε = 50												
1.0		21.86										
2.0		21.58										
3.0						18.09				15.12		
5.0	24.21	20.87	15.57	13.33	21.17	17.87	12.75	10.72	18.30	15.01	10.36	8.63
8.0		20.34				17.50				14.82		
10.0		20.12				17.29				14.68		
25.0	22.03	18.89	14.18	12.25	19.15	16.22	11.81	10.07	16.61	13.83	9.79	8.21

TABLE 9

KINETICS LOSS - RADIUS OF CURVATURE STUDY (Part 1)

	300#				3000#				18000#			
P_c / Rad of curv	50	100	300	500	50	100	300	500	50	100	300	500
ε = 75												
1.0		24.02										
2.0		23.73										
3.0						20.02				16.85		
5.0	26.74	22.99	17.19	14.82	23.51	19.79	14.17	12.02	20.44	16.74	11.60	9.76
8.0		22.50				19.41				16.54		
10.0		22.22				19.19				16.40		
25.0	24.47	20.93	15.74	13.69	21.4	18.07	13.19	11.35	18.68	15.51	11.02	9.36
ε = 100												
1.0												
2.0		25.2										
3.0						20.54				17.23		
5.0	27.83	24.44	17.83	15.57	24.47		14.67	12.65	21.27	17.12	11.99	10.28
8.0		23.93				19.92				16.92		
10.0		23.65				19.69				16.78		
25.0	25.49	21.52	16.34	14.41	22.3	18.54	13.68	11.96	19.47	15.86	11.40	9.87

TABLE 10

BELL NOZZLE KINETICS LOSSES

	300# Thrust											
	MR = 2.0				MR = 2.5				MR = 3.0			
P_c / % Bell	50	100	300	500	50	100	300	500	50	100	300	500
25/1 length												
80 (36.08)		13.933	8.768			21.502	16.552			18.59	13.397	
75 (40.34)						22.665	17.187				13.879	
70 (45.32)		15.03	9.355	7.05	25.79	23.350	17.822	15.42	20.73	19.64	14.261	
65 (51.75)		15.40	9.666		26.69	23.887	18.521	17.62	22.73	19.78	14.709	12.32
50/1 length												
80 (73.69)		16.239	10.136			26.316	20.087			21.484	15.563	
75 (83.08)		16.558	10.42			27.021	20.655	24.72		22.02	15.967	
70 (93.99)			10.702			27.747	21.218			22.476	16.367	
	3000# Thrust											
25/1 length												
80 (36.08)												
75 (41.74)												
70 (45.32)						20.16						
65 (51.75)					24.46	21.07	14.98	12.83				
80 (73.69)												
75 (83.08)												
70 (93.99)												

REFERENCES

1. Taylor, A. A. and Hoffman, J. D., "Design of Maximum Thrust Nozzles with Nonequilibrium, Chemically Reacting Flow", AFAPL-TR-71-92, Volume 1, December 1971.

2. Hoffman, J. D., "A. General Method for Determining Optimum Thrust Nozzle Contours for Chemically Reacting Gas Flows", AIAA j., 5, 4, April 1967, pp. 670-676.

3. Cline, M. C. and Hoffman, J. D., "An Investigation of the Analysis of Three-Dimensional Reacting Flows by the Method of Characteristics," Jet Propulsion Center, Purdue University, Report No. TM-69-6, November 1969.

4. Savili, V. J., Bender, L. S., and Bunwell, W. G., "Optimization of Nonequilibrium Nozzle Performance for Selected System Considerations", AIAA Preprint No. 69-472, June 1969.

5. Der, J. J., "Theoretical Studies of Supersonic Two-Dimensional and Axisymmetric Nonequilibrium Flow, Including Calculations of Flow through a Nozzle, "NASA Technical Report R-164, December 1963.

6. Frey, H. M. and G. R. Nickerson, "TDK Two-Dimensional Kinetic Reference Program", Dynamic Science, December 1970.

7. Powell, W. B., "Simplified Procedures for Correlation of Experimentally Measured and Predicted Thrust Chamber Performance", JPL Technical Memorandum 33-548, April 1, 1973. pp 20-23.

8. Penner, S. S., "Chemistry Problems in Jet Propulsion", Pergamon Press, NY. 1957. pp 216-217, 297-316.

AUTHOR'S BIOGRAPHY

FRED S. ANDES III, CAPT, USAF
AIR FORCE ROCKET PROPULSION LABORATORY

M.S., B.S. degree Mechanical Engineering, Texas A & M University (1963 - 1969).

Capt Andes specialized in the area of gas dynamics with general application to heat transfer and nuclear propulsion concepts. Thesis title: A Stability Analysis of Rotating Compressor Stall and its Application to Axial Flow Compressors. Thesis was application of Hamilton's principle of virtual work modified for a non-linear, non-conservative dynamic system under steady state oscillation.

Capt Andes has worked as a design engineer at the Cyclotron Institute under a research assistantship while at Texas A & M. For the past four years Capt Andes has served as a project engineer at the Air Force Rocket Propulsion Laboratory, Edwards AFB, California. During this time he has conducted complex experimental rocket research on highly classified foreign hardware and on advanced state-of-the-art nozzle design concepts.